QUANTITATIVE NEAR FIELD IMAGING WITH MULTI-DETECTOR WAVEGUIDE

R. Steegmüller and L. Diener
Institut für Kunststoffprüfung und Kunststoffkunde
Universität Stuttgart
Pfaffenwaldring 32
70569 Stuttgart / Germany

INTRODUCTION

Near field imaging with open ended waveguides has found increasing interest [1-3]. The basic idea is to scan across samples with a waveguide transducer as a reflection near field probe in order to characterize material properties and image defects that are much smaller than the wavelength. The reflection will form in the waveguide a standing wave where amplitude and phase depend on local intensity and phase of reflection. These effects can be demonstrated with slotted line measurements of the standing wave pattern. For example the investigations in figure 1 show the standing wave patterns for homogenous material and for a hidden hole. Depending on the material properties there is a change in phase and magnitude of the standing wave.

However, for imaging it is almost impossible to have such slotted line investigations for each scan position. Therefore often waveguide sensors with only one fixed detector are used where the detector is arranged at a highly sensitive position between the standing wave extrema. But such a probe cannot distinguish between changes in magnitude and phase. Also it is complicated to get quantitative results.
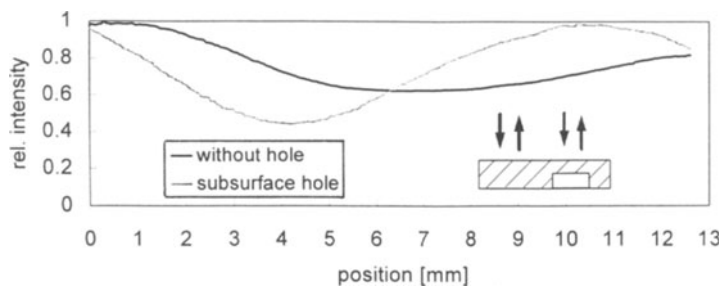

Figure 1. Slotted line measurement for homogenous material and hidden hole.

Review of Progress in Quantitative Nondestructive Evaluation, Vol 16
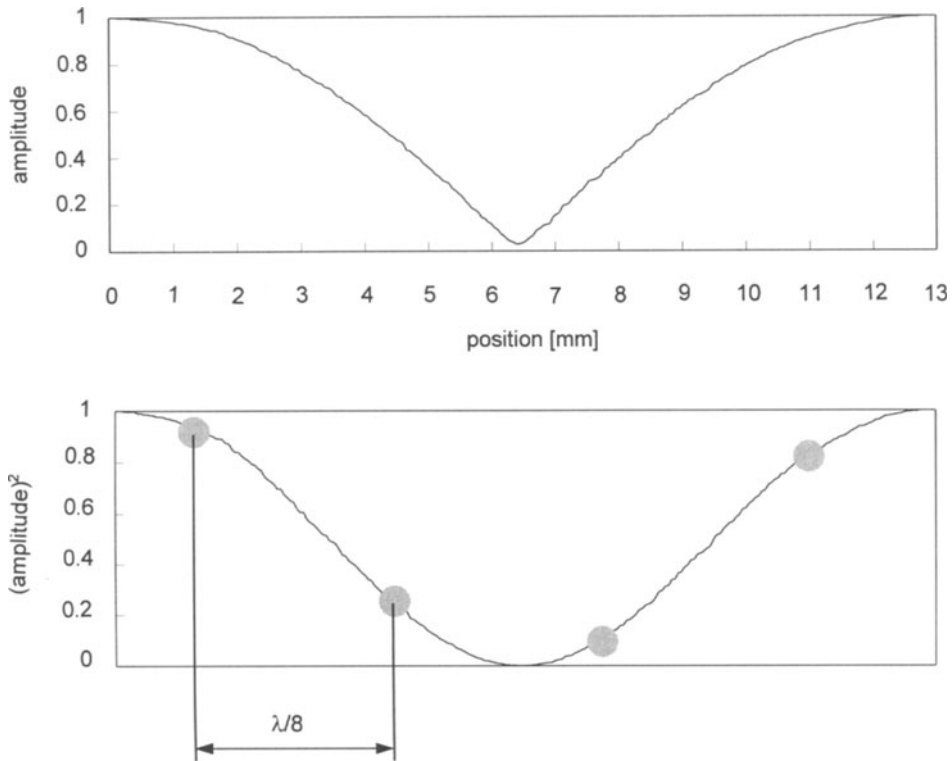Edited by D.O. Thompson and D.E. Chimenti, Plenum Press, New York, 1997

673

Figure 2. Amplitude of standing wave pattern (top), squared amplitude (intensity) curve (bottom), and detection positions for multi-detector principle.

THEORETICAL BACKGROUND AND EQUIPMENT

To overcome this limitation one can use an arrangement with three or more detectors in the waveguide with constant distances between them. This allows to analyse the phase and magnitude in a cheap way without using a network analyser. The basic idea is that the square of amplitude measured in the standing wave pattern should be a sinusoidal function (figure 2). Using simple Fourier algorithms one can calculate both phase and magnitude of this curve and therefore of the standing wave. Though three measured values are sufficient for such a procedure [4], in our measurements we used a four point algorithm because its simplicity allows for a fast calculation. The standing wave phase is

$$\varphi = arctan\frac{I_3 - I_1}{I_4 - I_5} \qquad (1)$$

while magnitude is

$$M = \sqrt{(I_3 - I_1)^2 + (I_4 - I_2)^2} \qquad (2)$$

where I_i (i=1-4) denote the squared amplitude at each detector.

Also we can determine the average of the squared amplitude and the standing wave ratio (SWR):

$$\bar{I} = \frac{I_1 + I_2 + I_3 + I_4}{4} \tag{3}$$

$$SWR = \sqrt{\frac{\bar{I} + M}{\bar{I} - M}} \ . \tag{4}$$

Our measurement transducer (figure 3) is built up with a 15 GHz microwave source, an open ended waveguide, and four detector diodes. These are arranged along the large side of the waveguide with constant distances of $\lambda/8$ (figure 2). The four detector signals allow for real time phase and magnitude calculation. In combination with a two dimensional raster scan this results in phase- and magnitude images.

RESULTS

At first we investigated a 3 mm thick PMMA-sample (figure 4) provided with hidden holes at depths between 2.5 mm and 0.5 mm and with diameters of 5 mm and 10 mm.
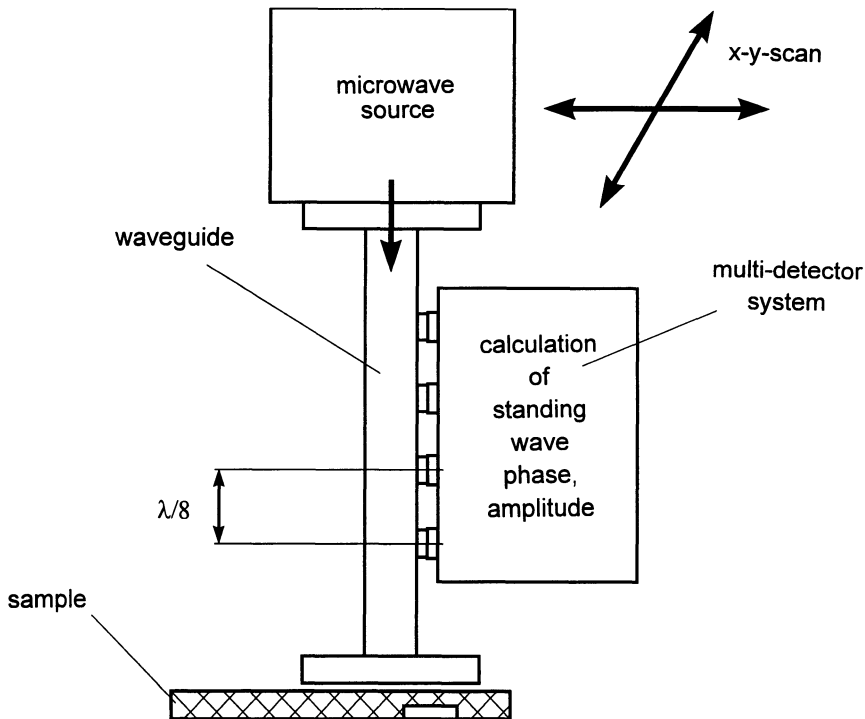

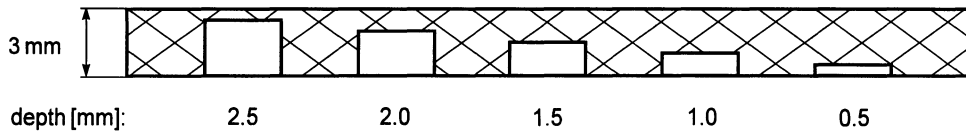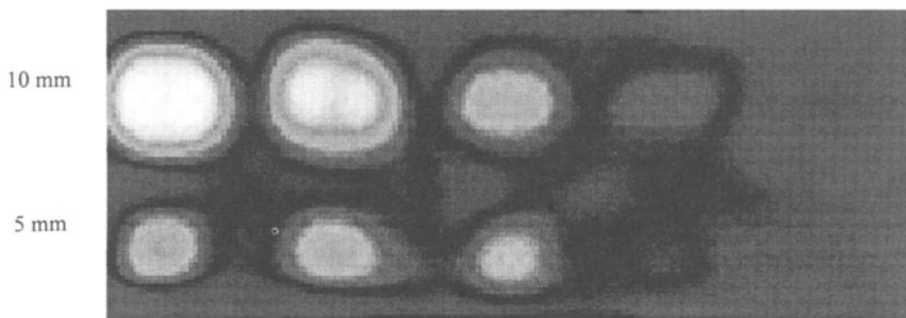
Figure 3. Four detector measurement transducer.

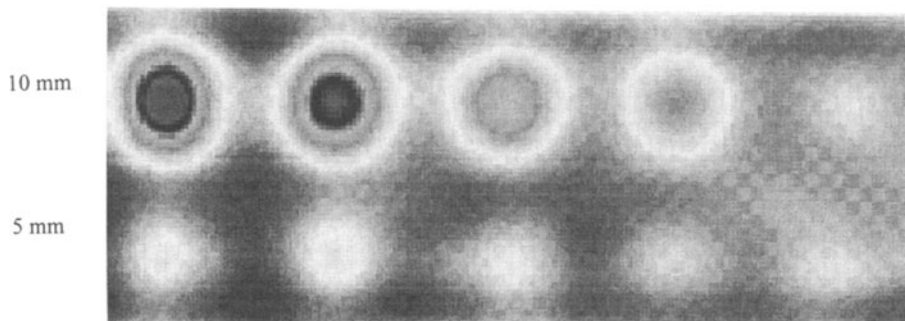Figure 4. PMMA-sample with hidden holes.

Figure 5 shows the magnitude and phase raster images of the PMMA-model sample. Obviously the resolution and imaging quality is much better with phase than with magnitude. We assume that the distortion of magnitude is an effect of the waveguide "point spread function" /2,5/.

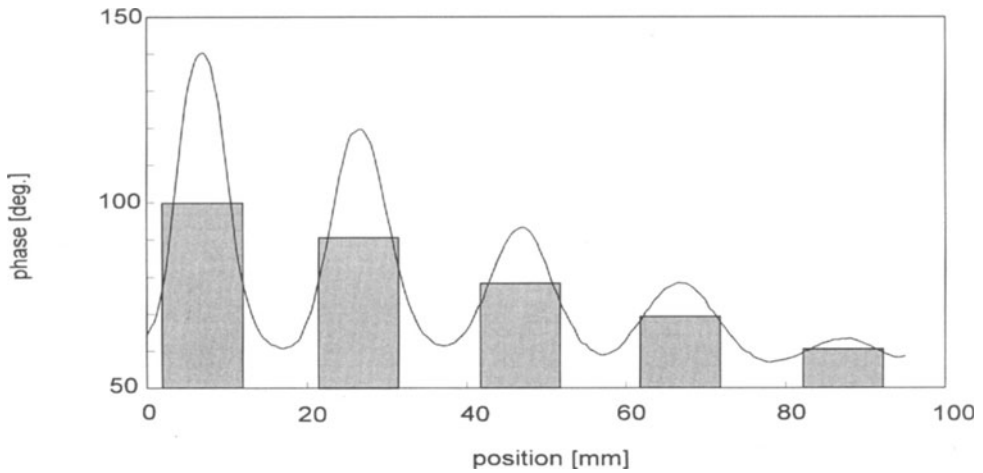Figure 5. Magnitude and phase image of PMMA-model sample.

Figure 6. Line scan with signal phase across the holes with 10 mm diameter in various depths.

The line scan (figure 6) through the phase image of holes with 10 mm diameter indicates a very high signal-to-noise ratio in the phase. Moreover this pattern fits reasonably well to the diameter and depths of the hidden holes. Also for the holes with 5 mm diameter the differences between phase maxima and minima correlate well with the hole depths (figure 7). Another interesting example of the advantages of phase and magnitude images obtained with our cheap four diode sensor is shown in figure 8. Here we investigated a veenered wood sample with hidden holes in the center, a hidden aluminium-foil in the right top corner and a knot in the left bottom corner. In the phase image all artifical defects are displayed but it is difficult to distinguish the knot and the foil. On the other side in the magnitude image one cannot find the knot. Also the holes are not so clear. However, the aluminum foil gives a strong signal due to the strong interaction of microwaves with metallic inclusions. So phase and magnitude imaging can be also helpful to characterize and distinguish different kinds of materials and defects.
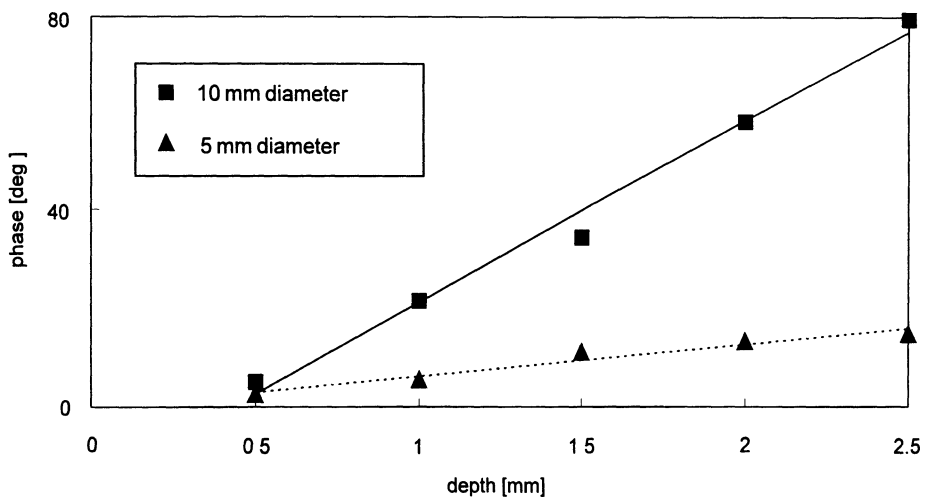

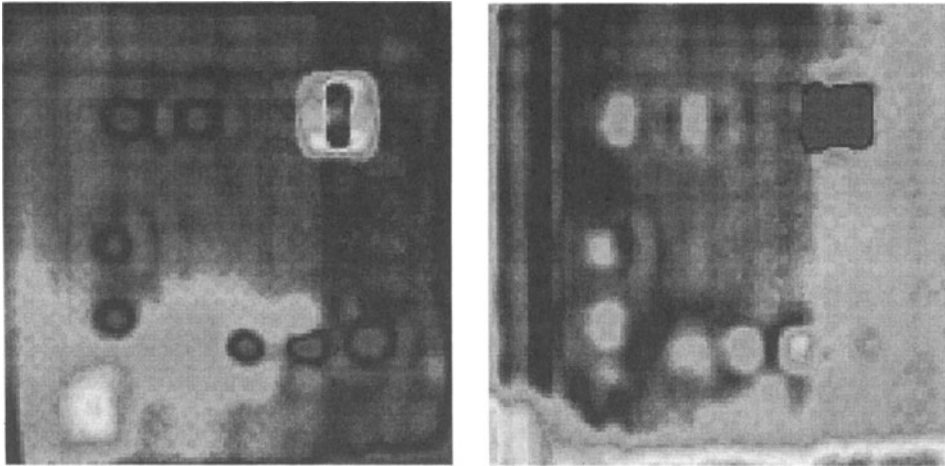Figure 7. Depth dependence of phase maxima in curve of figure 6.

Figure 8. Phase (left) and magnitude (right) images of a veenered wood with hidden defects.

CONCLUSION

It was shown how phase and magnitude of a standing wave can be analysed with a multi detector waveguide probe using a simple Fourier transform algorithm. The technique was used for two dimensional raster scan measurements to obtain phase and magnitude images. For two model samples with hidden holes and imbedded materials we demonstrated that phase and magnitude imaging can characterize defects and distinguish between material properties.

ACKNOWLEDGEMENTS

REFERENCES

1. S. Bakhitiari, S. Ganchev, and R. Zoughi, "Open-ended rectangular waveguide for nondestructive thickness measurement and variation detection of lossy dielectrics slabs backed by a conducting plate", in *IEEE Trans. Instrument Meas.* 42(1) (1993).
2. L. Diener, "Microwave near-field imaging with open-ended waveguide-comparison with other techniques of nondestructive testing", in *Research in Nondestructive Evaluation* (1995) 7:137-152.
3. M. Golosovsky, A. Galkin, and D. Davidov, "High-spatial resolution resistivity mapping of large-area YBCO films by a near-field millimeter-wave microscopy", in *IEEE Transactions on Microwave Theory and Techniques* 44(7) (1996).
4. W. J. Duffin, "Three-probe method of impedance measurement", in *Wireless Engineer*, December 1952.
5. L. Diener, R. Steegmüller, D. Wu, G. Busse, "Characterization of microwave near-zone field by using lockin-thermography", in *Science of China* (1996) (submitted).